
LATTICE DYNAMICS
AND PHASE TRANSITIONS

Optical and X-ray Diffraction Studies of the Symmetry of Distorted Phases of the $(\text{NH}_4)_3\text{ZrF}_7$ Crystal

S. V. Misyul^a, S. V. Mel'nikova^b, A. F. Bovina^b, and N. M. Laptash^c

^a Siberian Federal University, Svobodnyĭ pr. 59, Krasnoyarsk, 660041 Russia

e-mail: misjul@akadem.ru

^b Kirensky Institute of Physics, Siberian Division, Russian Academy of Sciences, Akademgorodok, Krasnoyarsk, 660036
Russia

^c Institute of Chemistry, Far East Division, Russian Academy of Sciences, pr. Stoletiya Vladivostoka 159, Vladivostok, 690022
Russia

Received January 28, 2008

Abstract— $(\text{NH}_4)_3\text{ZrF}_7$ single crystals were grown, and polarization-optical and x-ray diffraction studies were performed on powders and crystalline plates of various cuts over a wide temperature range. Phase transitions are revealed at temperatures $T_{1\uparrow} = 280$ K, $T_{2\uparrow} = 279.6$ K, $T_{3\uparrow} = 260$ – 265 K, and $T_{4\uparrow} = 238$ K on heating and at $T_{1\downarrow} = 280$ K, $T_{2\downarrow} = 269$ – 270 K, $T_{3\downarrow} = 246$ K, and $T_{4\downarrow} = 235$ K on cooling. The sequence of changes in symmetry is established to be as follows: O_h^5 ($Z = 4$) \longleftrightarrow D_{2h}^{25} ($Z = 2$) \longleftrightarrow C_{2h}^3 ($Z = 2$) \longleftrightarrow C_i^1 ($Z = 108$) \longleftrightarrow monoclinic² ($Z = 216$).

PACS numbers: 61.50.Ks, 64.70.Kb, 61.72.Mm

DOI: 10.1134/S1063783408100272

1. INTRODUCTION

Quantum-chemical calculations for compounds of heptafluorides of elements of the main subgroups with seven-coordinated complexes, such as TeF_7 , IF_7 , and XeF_7 , indicate that their geometry as pentagonal bipyramids is preferable. For heptafluorides of d^0 transition metals, the preferable geometry of such complexes (e.g., MoF_7 or WF_7) is a single-cap octahedron or a single-cap trigonal prism [1]. However, as early as 1954, for zirconium and hafnium heptafluoride compounds $A_3\text{Zr}(\text{Hf})\text{F}_7$ ($A = \text{NH}_4, \text{K}$), the pentagonal-bipyramidal structure of ZrF_7 and HfF_7 anions was proposed [2]. More recently, the proposed structure of the ZrF_7 anion in $(\text{NH}_4)_3\text{ZrF}_7$ was confirmed in [3, 4]. According to those data, at room temperature, $(\text{NH}_4)_3\text{ZrF}_7$ has an fcc structure (space group $O_h^5 - Fm\bar{3}m$, $Z = 4$) in which the pentagonal bipyramid ZrF_7 is disordered over 24 equivalent orientations. Two independent tetrahedral ammonium groups are also disordered. Based on the NMR data [5, 6], it was shown that the disorder in $(\text{NH}_4)_3\text{ZrF}_7$ and K_3ZrF_7 is dynamical. As the temperature decreases, these compounds undergo a structural transformation (in the range 235–213 K for ammonium and 254–224 K for potassium) from the cubic to orthorhombic structure. The NMR studies of the molecular motion and disorder

in K_3ZrF_7 [7] showed that the orthorhombic phase of K_3ZrF_7 is also disordered and that the molecular ion ZrF_7^{3-} has 16 possible orientations in the high-temperature cubic phase.

It should be noted that the refinement of the $(\text{NH}_4)_3\text{ZrF}_7$ structure [3, 4] in space group $O_h^5 - Fm\bar{3}m$ gives anomalously short F–F distances (2.15 Å) in the equatorial plane of the bipyramid. Because of this, in [8], the structure was refined in noncentrosymmetric space group $T^2 - F23$, which led to reasonable F–F contacts in the polyhedron. In this case, ZrF_7^{3-} has six independent orientations and one of the three crystallographically independent ammonium groups in the structure is disordered over six or twelve equivalent orientations. An attempt to determine the crystal structure of the low-temperature distorted phase of $(\text{NH}_4)_3\text{ZrF}_7$ in [8] using x-ray diffraction have failed owing to a complex twinning.

In this work, we performed polarization-optical and x-ray diffraction studies and measured the rotation angle of the optical indicatrix of the $(\text{NH}_4)_3\text{ZrF}_7$ crystal over a wide temperature range (80–450 K) with the aim of searching phase transitions (PTs) and determining the phase symmetry.

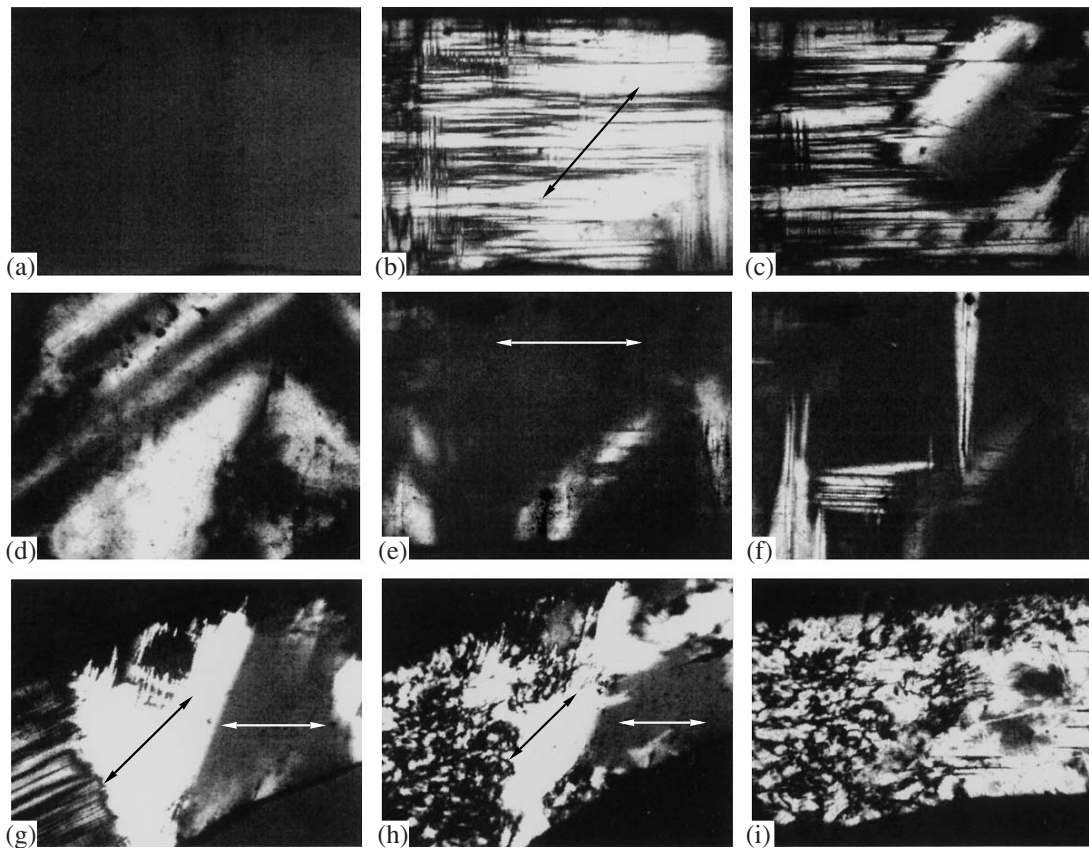


Fig. 1. Images of a $(100)_c$ -cut plate in polarized light (a–c; g–i) immediately after the sample treatment and (d–f) after two days of storage: (a) at room temperature (G_1 phase); (b, d, e) the G_2 phase (extinction along $[100]_c$ and $[110]_c$); (c, f) appearance of G_3 -phase front; (g) the G_3 phase (the optical indicatrix is rotated in neighboring twins by $\pm\varphi$); (h) the G_4 phase (coexistence of twins with large ($\pm\varphi$) and small ($\pm\psi$) misorientation angles from $[100]_c$); and (i) transformation of the twin structure in the G_5 phase.

2. EXPERIMENTAL RESULTS

$(\text{NH}_4)_3\text{ZrF}_7$ single crystals were synthesized in the form of well-faceted octahedra from fluoride aqueous solutions of zirconium oxides in HF with an excess of NH_4F . The crystallization was carried out on slow evaporation of a saturated solution in air at room temperature. It should be noted that, according to the chemical analysis data, the $(\text{NH}_4)_3\text{ZrF}_7$ crystal composition was not completely stoichiometric owing to a partial isomorphic replacing of the fluoride ion by hydroxide. Their actual composition is $(\text{NH}_4)_3\text{Zr}(\text{OH})_x\text{F}_{7-x}$ (on average, $x = 0.3$). The fluorine content was determined by distillation in the form of H_2SiF_6 followed by the titration with $\text{Th}(\text{NO}_3)_4$ and using a fluorine-selective electrode. In what follows, we use the stoichiometric formula $(\text{NH}_4)_3\text{ZrF}_7$.

The x-ray diffraction study of the $(\text{NH}_4)_3\text{ZrF}_7$ crystal was performed using a DRON-2.0 diffractometer equipped with an URNT-180 low-temperature attachment ($\text{Cu } K_\alpha$ radiation, graphite monochromator). The polarization-optical measurements were carried out using an Axiolab polarizing microscope. As samples,

we used single-crystal plates of $(100)_c$, $(110)_c$, and $(111)_c$ cuts and also powders obtained from $(\text{NH}_4)_3\text{ZrF}_7$ single crystals (here and in what follows, the indices of planes, directions, and x-ray reflections correspond to the parameters of the cubic G_1 phase).

The study performed in polarized light shows that, at room temperature, the crystal does have cubic symmetry (the G_1 phase; Fig. 1a). On cooling, at a temperature somewhat higher than the ice-thawing temperature, the crystal becomes optically anisotropic and is divided into polysynthetic twins. A second-order PT occurs accompanied by a change in the crystal system. In a plate cut along $(100)_c$ (octahedron vertex) studied immediately following the treatment, this transition occurs at a temperature $T_\downarrow = 280$ K and is accompanied by the appearance of band twins with boundaries along the $[110]_c$ direction and by the extinction of the entire system in the $[100]_c$ direction (Fig. 1b). After storage for one to two days, the twin structure is changed over this temperature range (Fig. 1d). Twins with diffuse interfaces in the $[110]_c$ direction and with extinction in them in the $[110]_c$ direction (Fig. 1e) are dominant, but the previous twin structure is also present.

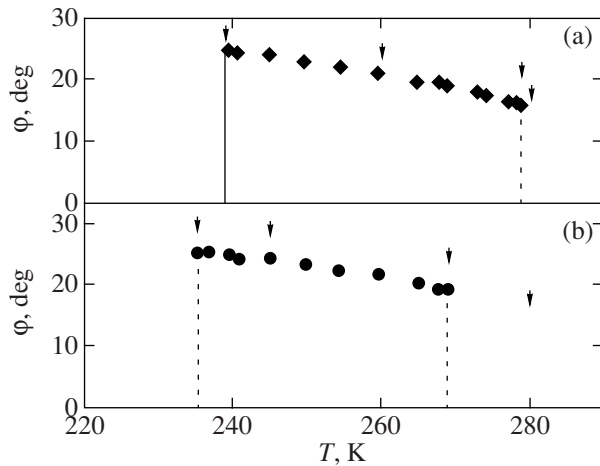


Fig. 2. Temperature dependence of the rotation angle $\varphi(T)$ of the optical indicatrix with respect to the $[100]_c$ direction. (a) Heating: $T_{1\uparrow} = 280$ K, $T_{2\uparrow} = 279.6$ K, $T_{3\uparrow} = 260$ – 265 K, and $T_{4\uparrow} = 238$ K. (b) Cooling: $T_{1\downarrow} = 280$ K, $T_{2\downarrow} = 269$ – 270 K, $T_{3\downarrow} = 246$ K, and $T_{4\downarrow} = 235$ K. Owing to large thermal hysteresis of the transition at T_2 , the range of existence of tetragonal phase G_2 narrows to 0.5 K on heating.

As the temperature decreases, a new phase is nucleated at $T_{2\downarrow} = 269$ – 270 K; the nucleation is accompanied by the motion of the phase front in the sample both after the treatment (Fig. 1c) and after the storage (Fig. 1f). The completely formed twin pattern (Fig. 1g) differs sharply from the previous one (Fig. 1b). We see two large twins in which the extinctions differ by $\pm 2\varphi \approx 40^\circ$. The angle φ is reckoned from the $[100]_c$ direction of the cubic unit cell. The extinction in the sample region with small band twins occurs in the $[010]_c$ direction. At a temperature $T_{3\downarrow} = 246$ K, the twin pattern is also changed (predominantly in the region of small twins). The optical indicatrix is somewhat disoriented by $\pm\psi \approx 2^\circ$ with respect to the $[100]_c$ direction (Fig. 1h). During further cooling, one more temperature ($T_{4\downarrow} = 235$ K) is revealed at which the twin pattern is completely changed. The optical anisotropy increases sharply, a color appears, and the extinction position in twins is changed (Fig. 1i). We see good extinction in the $[100]_c$ direction in one series of twins and a small misorientation of the extinctions along $[110]_c$ in another.

The examination of the $[111]_c$ cut in polarized light revealed that the threefold axis of the crystal is lost in the phase transition at $T_{1\downarrow}$ and, below this temperature, a characteristic structure is formed with three types of twin interfaces oriented at an angle of 120° to each other.

Figure 2 shows the temperature dependence of the rotation angle of the optical indicatrix $\varphi(T)$ on cooling and heating. The PTs at T_2 and T_4 are accompanied by a stepwise appearance and disappearance of the angle $\varphi(T)$

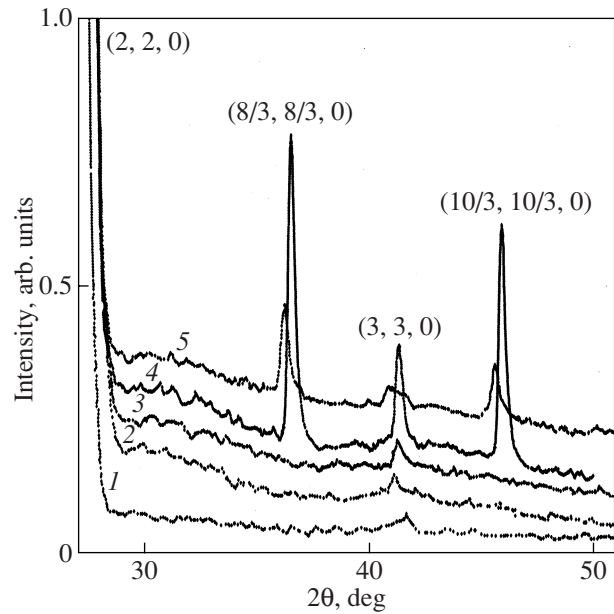


Fig. 3. Fragments of the x-ray diffraction patterns from a $(100)_c$ -cut plate of the $(\text{NH}_4)_3\text{ZrF}_7$ crystal in the (1) G_1 , (2) G_2 , (3) G_3 , (4) G_4 , and (5) G_5 phases.

and are characterized by a significant thermal hysteresis. The PT temperatures are as follows: $T_{1\uparrow} = 280$ K, $T_{2\uparrow} = 279.6$ K, $T_{3\uparrow} = 260$ – 265 K, and $T_{4\uparrow} = 238$ K.

The room-temperature powder x-ray diffraction pattern shows the x-ray reflections corresponding to space group $O_h^5-Fm\bar{3}m$ ($Z = 4$) with a fluorine fcc unit cell. However, among the reflections from single-crystal plates, additional weak reflections of the $(h, h, 0)_c$ type with odd indices h were unexpectedly revealed. (The reflection indices h, k, l are defined with respect to the unit cell axes of the G_1 cubic phase.) On cooling, the intensities of these lines remain practically unchanged down to T_3 and then, below T_3 , they increase substantially (Fig. 3). Moreover, below this temperature, a system of superstructure reflections of the $(h \pm 1/3, h \pm 1/3, 0)_c$ type arises (h is an odd integer). These superstructure reflections retain below T_4 with somewhat changed intensities. Figure 4 shows the temperature dependence of the $(3 - 1/3, 3 - 1/3, 0)_c$ superstructure reflection intensity measured on heating. This dependence has two specific features at $T_{3\uparrow}$ and $T_{4\uparrow}$. In the range between $T_{3\uparrow}$ and $T_{4\uparrow}$, the intensity of this reflection is far higher than that in the low-temperature phase.

The profiles of the x-ray reflections from the single-crystal plate are significantly changed as the temperature decreases. Their splittings in all the phases observed are shown schematically in the table. The table also lists the linear and angular crystal unit cell parameters of various phases found from the positions of the $(6, 6, 0)_c$ reflection components.

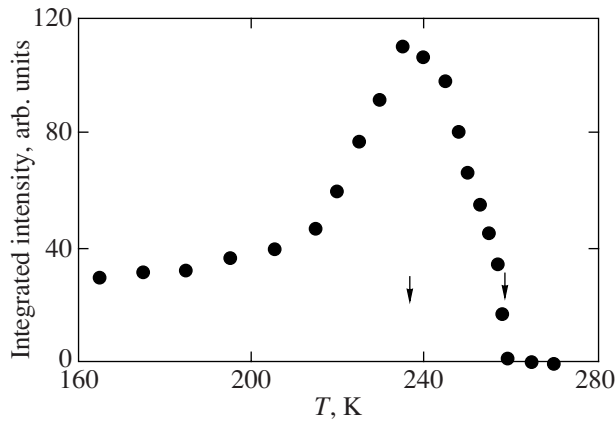


Fig. 4. Temperature dependence of the integrated intensity of superstructure reflection $(8/3, 8/3, 0)$ in the G_4 and G_5 phases measured on heating. The arrows indicate the phase transition temperatures.

3. DISCUSSION OF THE RESULTS

In this study, we have shown that the $(\text{NH}_4)_3\text{ZrF}_7$ crystal becomes optically anisotropic and, below room temperature, the following sequence of PTs occurs: cubic (G_1) \longleftrightarrow orthorhombic (G_2) \longleftrightarrow monoclinic¹ (G_3) \longleftrightarrow triclinic (G_4) \longleftrightarrow monoclinic² (G_5) phase. Note that the splittings of the x-ray reflections $(h, 0, 0)_c$ and $(h, h, 0)_c$ in the G_2 orthorhombic phase correspond to the tetragonal symmetry. This result is due to very small distortions, for which the orthorhombic unit cell is fairly close to the tetragonal one.

In determining the groups of symmetry of the low-temperature crystal phases, the following established facts are important. (1) The $G_1 \longleftrightarrow G_2$ PT is smooth (second order). (2) The $G_2 \longleftrightarrow G_3$ PT is accompanied by motion of the phase front and a jump in the rotation angle of the optical indicatrix; i.e., it is of first order. (3) According to the extinctions in polarized light, the unit cell of the orthorhombic phase G_2 is oriented so that the $[001]_c$ direction coincides with the fourfold axis of the cubic phase and the two other crystallographic directions are along $[110]_c$. (4) The principal axes of the unit cells of the G_3 and G_4 phases are parallel to those of the cubic unit cell. (5) In monoclinic phase G_5 , the specific direction coincides with $[100]_c$ and the two other directions are parallel to $[110]_c$. (6) In the G_3 and G_4 phases, the rotation angle of the optical indicatrix $\varphi(T)$ is large, which is characteristic of intrinsic ferroelastic phase transitions for which the spontaneous deformation x_6 is the order parameter of the transition. (7) In the G_4 and G_5 phases, there are superstructure x-ray reflections indicating a change in the crystal translation symmetry. The determination of the room-temperature space group of the crystal (phase G_1) is of importance in determining the sequence of changes in

symmetry due to the PTs. The experimental data suggest three variants of the G_1 phase symmetry.

First, the presence of weak reflections $(3, 3, 0)_c$ (Fig. 3) revealed in this work might indicate that the Bravais cell of the cubic phase is face-centered and we initially assumed that the space group is $O_h^4 - Pn\bar{3}m$. However, the fact that their intensity remains practically unchanged in the G_1, G_2 , and G_3 phases and is several orders of magnitude lower than the intensity of the main structure reflections and that degradation of the sample surface (observed under microscope) occurs over the course of time allows the assumption that these phenomena are likely due to surface-layer distortions. This conclusion is supported by the circumstance that the penetrability of the $\text{CuK}\alpha$ radiation used in our experiments is small and, thus, the results of the x-ray diffraction measurements are sensitive to the surface-layer state.

Another variant of the room-temperature crystal symmetry is $O_h^5 - Fm\bar{3}m$ [3, 4]. Based on the changes in the intensities of the superstructure reflections in the various phases (Fig. 3), we may assume that the $(h, h, 0)_c$ reflections appear along with the $(h \pm 1/3, h \pm 1/3, 0)_c$ reflections (h is an odd integer) in the G_4 triclinic phase. It means that the transitions $G_1 \longleftrightarrow G_2 \longleftrightarrow G_3$ in the $(\text{NH}_4)_3\text{ZrF}_7$ crystal occur without changing the translational symmetry. The large rotation angle $\varphi(T)$ of the optical indicatrix in the monoclinic phase G_3 is characteristic of intrinsic ferroelastic transitions, which are also not accompanied by a change in the unit cell volume. Based on group-theory analysis [9], the most probable sequence of transitions $G_1 \longleftrightarrow G_2 \longleftrightarrow G_3 \longleftrightarrow$

$G_4 \longleftrightarrow G_5$ can be interpreted as follows: $O_h^5 \xrightarrow{(0, 0, c_1)} D_{2h}^{25} \xrightarrow{(0, c_1, c_1)} C_{2h}^3 \longleftrightarrow C_i^1 \longleftrightarrow$ monoclinic² phase (see table). The transition three-component order parameter indicated above the arrows is transformed according to irreducible representation (IR) 11-9 corresponding to the Γ point ($K11$) in the Brillouin zone center. We use the notation for IRs introduced in handbook [10]. This sequence of changes in the symmetry of the $(\text{NH}_4)_3\text{ZrF}_7$ crystal with decreasing temperature does not contradict the experimental results. The appearance of the $(h \pm 1/3, f \pm 1/3, 0)_c$ reflections in the G_4 phase indicates a threefold increase of the unit cell in size along the crystallographic axes of cubic phase G_1 , which is unusual for such crystals and requires additional studies. We determine the symmetry of this phase using the results of the polarization-optical measurements, which indicate that the optical indicatrix is rotated with respect to all crystallographic directions of the cubic phase. Out of the two space groups of the triclinic crystal system, we choose space group $G_i^1 - P\bar{1}$ with a center of inversion and with unusual changes in the unit cell parameters. The space group of the monoclinic phase G_5 can-

Crystallographic characteristics of distorted phases of the $(\text{NH}_4)_3\text{ZrF}_7$ crystal

	G_5	G_4	G_3	G_2	G_1
Space group	Monoclinic ²	$C_i^1-P\bar{1}$	C_{2h}^3-I2/m	$D_{2h}^{25}-Immm$	$O_h^5-Fm\bar{3}m$
Z	216	108	2	2	4
T_{exp} , K	223	245	267	280	295
Bravais unit cell parameters					
\mathbf{a}_i , Å	$3(\mathbf{a}_1 + \mathbf{b}_1)$ 39.164	$(3\mathbf{a}_1)$ 28.180	$1/2(\mathbf{a}_1 + \mathbf{b}_1)$ 6.614	$1/2(\mathbf{a}_1 + \mathbf{b}_1)$ 6.654	(\mathbf{a}_1) 9.415
\mathbf{b}_i , Å	$3(\mathbf{a}_1 - \mathbf{b}_1)$ 39.776	$(3\mathbf{b}_1)$ 28.156	$1/2(\mathbf{a}_1 - \mathbf{b}_1)$ 6.607	$1/2(\mathbf{a}_1 - \mathbf{b}_1)$ 6.654	(\mathbf{b}_1) 9.415
\mathbf{c}_i , Å	$(3\mathbf{c}_1)$ 27.880	$(3\mathbf{c}_1)$ 28.037	(\mathbf{c}_1) 9.440	(\mathbf{c}_1) 9.342	\mathbf{c}_1 9.415
α , deg	90	90.120	90	90	90
β , deg	90	89.889	90	90	90
γ , deg	89.879	89.913	89.866	90	90
V , Å ³	43431.10	22245.54	412.52	413.61	834.57
Scheme of splittings of reflections					
$(h\ 0\ 0)$					
$(h\ h\ 0)$					
$(h\ h\ h)$					
Superstructure	Exists	Exists	No	No	No

not be determined because the obtained x-ray diffraction data are limited. Note that the direction of the twofold axis is the same in all monoclinic phases.

As a third variant of the room-temperature crystal symmetry, we consider noncentrosymmetric group T^2-F23 proposed in [8], which is a subgroup of space group $O_h^5-Fm\bar{3}m$. This fact permits us to assume the occurrence of a PT at higher temperatures, namely, $F23 \longleftrightarrow Fm\bar{3}m$ (phase G_0). A group theoretical analysis [9] and a study of the complete condensate of order parameters (OPs) [11] show that this phase transition can occur only in the case where two one-component OPs interact transforming according to the 11-2 and 11-4 IRs of space group $O_h^5-Fm\bar{3}m$. In this case, as follows from an analysis of the permutation and mechanical representations of crystals with symmetry $O_h^5-Fm\bar{3}m$ [11], the 11-2 OP is associated with the displacement of the F and H atoms and the 11-4 OP is related to the ordering of these atoms.

For the case of interacting one-component OPs, the thermodynamic potential describing the phase diagram was considered in [12] and its detailed analysis is given in [13]. Based on the results from [9, 13], one can conclude that second-order phase transitions from $O_h^5-Fm\bar{3}m$ can occur along a line on the phase diagram only to phases with symmetries O^3-F432 (IR 11-2) or $T_d^2-F\bar{4}3m$ (IR 11-4). A second-order PT to T^2-F23 is also possible but only either through intermediate phases or at a point on the phase diagram. The direct $Fm\bar{3}m \longleftrightarrow F23$ transition along a line between the phases occurs only as a first-order transformation. We searched such a transition on heating from room temperature to the crystal decomposition temperature (~400 K) but failed to find it.

Now consider the sequence of changes in symmetry that occurs with decreasing temperature. The above experimental results indicate that the $G_1 \longleftrightarrow G_2$ PT is of second order. Moreover, the studies of the twin structure in the G_2 phase revealed with confidence that the

axes of the orthorhombic unit cell are arranged at an angle of 45° to $[100]_c$, which corresponds to space group $D_{2h}^{25}-Immm$. It is not a subgroup of the T^2-F23 group, and, thus, the $F23-Immm$ transition must occur jumpwise (as a first-order transition).

The further symmetry lowering $G_3 \longleftrightarrow G_4 \longleftrightarrow G_5$ is described by the sequence presented in the table. In this case, the crystal “forgets” the symmetry of the G_1 and G_2 phases during the $G_2 \longleftrightarrow G_3$ transition. This conclusion is confirmed by the fact that the G_3 phase is nucleated in the G_2 phase as a front that erases the memory of the twin structure of the previous phase. Thus, if space group T^2-F23 describes the symmetry of the G_1 phase, then it is difficult to construct the chain of changes in symmetry due to PTs that occur in $(\text{NH}_4)_3\text{ZrF}_7$ as the temperature decreases. Because of the absence of group-subgroup relations between G_1 and G_2 , the smooth transition between these phases cannot be explained.

4. CONCLUSIONS

All experimental data clearly show that $O_h^5-Fm\bar{3}m$ is the most probable symmetry of the room-temperature phase of the $(\text{NH}_4)_3\text{ZrF}_7$ crystal. This variant is also supported by the octahedral habitus of the crystal and the absence of optical second harmonic generation, which we have tested on powder samples using an infrared laser. The studies have revealed a complex sequence of phase transitions: cubic (G_1) \longleftrightarrow orthorhombic (G_2) \longleftrightarrow monoclinic¹ (G_3) \longleftrightarrow triclinic (G_4) \longleftrightarrow monoclinic² (G_5) phase, which occur in the $(\text{NH}_4)_3\text{ZrF}_7$ crystal in the temperature range 280–238 K. The supposed space groups of some phases of this material are shown in the table. These results confirm the occurrence of the structural transformations in the crystal assumed previously in [5, 6], where, however, only the lowest-temperature transition to the G_5 phase was detected and this phase was assigned to the orthorhombic crystal system.

ACKNOWLEDGMENTS

We are grateful to A.S. Aleksandrovskii for his assistance in performing the experiments on optical second harmonic generation.

This work was supported by the Council on Grants from the President of the Russian Federation (project NSh-4137.2006.2).

REFERENCES

1. Z. Lin and I. Bytheway, *Inorg. Chem.* **35**, 594 (1996).
2. W. H. Zachariasen, *Acta Crystallogr.* **7**, 792 (1954).
3. H. J. Hurst and J. C. Taylor, *Acta Crystallogr., Sect. B: Struct. Crystallogr. Cryst. Chem.* **26**, 417 (1970).
4. H. J. Hurst and J. C. Taylor, *Acta Crystallogr., Sect. B: Struct. Crystallogr. Cryst. Chem.* **26**, 2136 (1970).
5. V. P. Tarasov and Yu. A. Buslaev, *Zh. Struct. Khim.* **10**, 930 (1969).
6. Yu. A. Buslaev, V. I. Pakhomov, V. P. Tarasov, and V. N. Zege, *Phys. Status Solidi B* **44**, K13 (1971).
7. E. C. Reynhardt, J. C. Pratt, A. Watton, and H. E. Petch, *J. Phys. C: Solid State Phys.* **14**, 4701 (1981).
8. N. M. Laptash and A. A. Udovenko, in *Abstracts of Papers of the 15th European Symposium on Fluorine Chemistry, Prague, Czech Republic, 2007* (Prague, 2007), p. 126.
9. V. I. Zinenko and S. V. Misyul', Available from VINITI, No. 313-78 (1978).
10. O. V. Kovalev, *Irreducible and Induced Representations and Corepresentations of the Fedorov's Groups* (Nauka, Moscow, 1986) [in Russian].
11. K. S. Aleksandrov, S. V. Misyul, and E. E. Baturinets, *Ferroelectrics* **354**, 60 (2007).
12. E. M. Lifshitz, *Zh. Éksp. Teor. Fiz.* **14**, 353 (1944).
13. Yu. A. Izyumov and V. N. Syromyatnikov, *Phase Transitions and Crystal Symmetry* (Nauka, Moscow, 1984; Kluwer, Dordrecht, 1990).

Translated by Yu. Ryzhkov